

Optimization of photovoltaic thermal (PV/T) hybrid collectors by genetic algorithm in Iran's residential areas

Behzad Farshin^{2a} and M. A. Ehyaei^{*1}

¹Department of Mechanical Engineering, Pardis Branch, Islamic Azad University, Pardis New City, Iran

²Department of Mechanical Engineering-Energy Conversion, Islamic Azad University, Boroujerd Sciences and Researches Branch, Iran

(Received January 5, 2017, Revised April 18, 2017, Accepted April 19, 2017)

Abstract. In the present study, PV/T collector was modeled via analysis of governing equations and physics of the problem. Specifications of solar radiation were computed based on geographical characteristics of the location and the corresponding time. Temperature of the collector plate was calculated as a function of time using the energy equations and temperature behavior of the photovoltaic cell was incorporated in the model with the aid of curve fitting. Subsequently, operational range for reaching to maximal efficiency was studied using Genetic Algorithm (GA) technique. Optimization was performed by defining an objective function based on equivalent value of electrical and thermal energies. Optimal values for equipment components were determined. The optimal value of water flow rate was approximately 1 gallon per minute (gpm). The collector angle was around 50 degrees, respectively. By selecting the optimal values of parameters, efficiency of photovoltaic collector was improved about 17% at initial moments of collector operation. Efficiency increase was around 5% at steady condition. It was demonstrated that utilization of photovoltaic collector can improve efficiency of solar energy-based systems.

Keywords: solar energy; PV/T collector; photovoltaic cell; genetic algorithm; optimization

1. Introduction

The technologies related to renewable energies met for nearly 13.3% of primary global energy demand (Alekklett *et al.* 2010). During the successive years, numerous researchers have conducted activities across the world for benefiting from clean solar energy. The major reasons of such activities are world problems like global warming, rise in oil and gas costs, and predictions that non-renewable energy resources will be run out within the future 50 to 100 years. Statistical forecasts of International Energy Agency (IEA) regarding the world's petroleum reveal that production of crude oil and oil products are expanding and increasing and a reduction would take place in global oil consumption up to 2030 (Alekklett *et al.* 2010). The researchers regard air contamination resulting from production and consumption of fossil fuels as the primary cause of global warming. Fossil fuels and their associated pollution lead to environmental issues such as

*Corresponding author, Ph.D., E-mail: aliehyaei@yahoo.com

^aM.S. Student

acid rains and greenhouse effect. Currently, utilization of new and renewable energies has been commenced and this process has turned into a symbolic approach in many countries. Solar energy is among the accessible and inexpensive sources of energy that can serve as a suitable alternative for this purpose. As an endless source of energy, sun can partially solve the problems existing in the field of energy and environment conservation. The advantages of this energy resource include its cleanness and availability and the disadvantages are its temporary state, low potential, and requirement for large absorption plates (Lonngren and Bai 2008).

Nowadays, solar energy can be converted into thermal and/or electrical energies using the available technologies. The most common systems used for converting solar energy into thermal energy are collectors with water as the fluid. These systems have been developed for many years in numerous countries and solar energy is converted into electrical energy via photovoltaic cells. During energy conversion process in the respective cells, the thermal energy of sunlight is absorbed into the cell due to direct exposure to the solar radiation and also inherent color of the cells. This thermal energy causes the cell temperature to rise and reduces its energy conversion efficiency. Under normal conditions, part of this energy is transferred to the environment but cell temperature rises to such a level that a considerable decline is observed in its efficiency. The following equation represents effect of temperature on efficiency of photovoltaic cell (Duffie and Beckman 1991)

$$\eta_{mp} = \eta_{mp,ref} + \mu_{n,mp}(T_c - T_{ref}) \quad (1)$$

Where, η_{mp} is cell efficiency at point of maximum power, $\eta_{mp,ref}$ is cell efficiency point of maximum power under reference conditions (reference radiation intensity and temperature), $\mu_{n,mp}$ is temperature coefficient of photovoltaic cell efficiency (K^{-1}), T_c is operation temperature of photovoltaic cell, and $T_{ref}=25^\circ C$ is reference temperature. Cooling the cell is the solution proposed to prevent from such efficiency impairment. This is done by flowing a fluid such as air or water in the cooling system installed beneath the photovoltaic cell. As such, the surplus thermal energy of the cell is converted into effective thermal energy. Therefore, solar energy is simultaneously converted to electrical and thermal energies and overall energy conversion efficiency is also increased. All these processes are included in an ensemble designated as thermo-photovoltaic system. PV/T collectors have the following advantages compared to ordinary solar collectors (Aste *et al.* 2014)

- Efficiency improvement of photovoltaic module thanks to heat absorption from its plate by means of the fluid flowing in the solar collector
- Utilization of optimal installation space due to combination of solar collector and photovoltaic module
 - Greater durability of cells due to temperature reduction
 - Cogeneration electricity and heat
 - Return of equity in a shorter duration

During the recent years, various kinds of thermo-photovoltaic systems have been designed and analyzed by the researchers. Aste *et al.* (2014) extensively investigated flat-plate PV/T collectors which are mainly used in the market. They carried out numerous studies on identification of principal designing parameters of the respective collectors (Aste *et al.* 2014). Ebrahim *et al.* categorized, designed, and assessed performance of flat-plate PV/T collectors with water, air and both fluids as cooling fluid. They compared and discussed different designs of features and performance of flat-plate PV/T solar collector for use in residential and commercial buildings.

They concluded that utilization of this technology was promising and could lead to reduction of energy consumption (Ibrahim *et al.* 2011). Agrawal and Tiwari investigated energy and exergy analysis of a hybrid micro-channel photovoltaic thermal with constant mass flow rate. Thermal system was modeled with constant mass flow rate. Due to research results, thermal and exergy efficiencies increased 70.62% and 60.19%, respectively (Agrawal and Tiwari 2011). Tyagi *et al.* (2012) reviewed recent progresses in the scope of PV/T collectors. They presented research and development trend of technology progress in photovoltaic/ thermal (PV/T) cells and their practical programs. They proposed a new designing method aimed at enhancing effectiveness of thermal energy at lowest cost in comparison with ordinary hybrid collector technology. Empirical results were analogous to theoretical predictions suggesting that performance of new PV/T collector is better than the previous ordinary PV/T collectors (Tyagi *et al.* 2012). Baker *et al.* (2013) attempted to improve design of PV/T collectors for simultaneous heating of water and air. They formulated energy balance equations for both fluids and checked validity of this model and its application for a wide range of mass flow rates. Performance of the collector was also tested in the situation when the fluids are used independently. Their research results indicated that collector performed better when air and water are used simultaneously (Bakar *et al.* 2013). Moradi analyzed major impact of control parameters on PV/T collectors and also design of such collectors, providing a general outline of the performance improvement of PV/T collectors through applying the respective parameters. He analyzed the constituting materials of photovoltaic module and their improvement. Efficiency of collectors was the almost significant parameter in his research and he presented productivity tables for other researchers and designers (Moradi and Ebadian 2013). Kroib *et al.* (2014) developed a PV/T water purifier with the aim of reducing expenses and improving performance of thermal and electrical efficiencies (Kroib *et al.* 2014). Jang *et al.* simulated a PV/T collector using TRANSYS software. In the respective research, they optimized tank volume and collector inclination and compared numerical results with empirical data. Their research results showed that the highest efficiency was 67.5% for tank volume of 80 liters, and, annual efficiency improvement was around 4.37% and the cumulative absorbed heat is 2328 MJ (Kroib *et al.* 2014). Sobhnamayan *et al.* (2014) considered optimization of solar cogeneration system which is a combination of solar collector and photovoltaic cells. After electrical and thermal modeling, they used genetic algorithm to optimization of mentioned system. Their data has a good agreement with experimental data. They also obtained optimized variable such as inlet water velocity (0.09 m/s) and pipe diameter (4.8 mm), respectively (Sobhnamayan *et al.* 2014).

Rajab developed and optimized numerical solution of a PV/T collector for application in semiarid climate. He evaluated the monthly thermal and electrical energies by developing a mathematical model to determine dynamic behavior of PV/T collector based on energy balance between six main components of collector i.e., transparent layer, PV module, absorber plate, tubes, fluid inside the tubes, and insulator. Comparison of simulated results to empirical findings corroborate that the proposed model was practically applicable (Rejab *et al.* 2015).

Gou *et al.* (2015) assessed air and water-based PV/T collectors and developed the model for the steady and dynamic state. Accordingly, collector performance was analyzed under different flow rates, wind speed, and input water and air temperature. It was shown that efficiency of PV/T collector with water was higher than with air (Guo *et al.* 2015). Saeedi *et al.* (2015) optimized PV/T collector. They improved energy productivity via analyzing and formulating energy balance equations for different parts of collectors and benefitted from computer simulation in order to obtain the thermal and electrical parameters taking into account different operational parameters in energy efficiency (Saeedi *et al.* 2015).

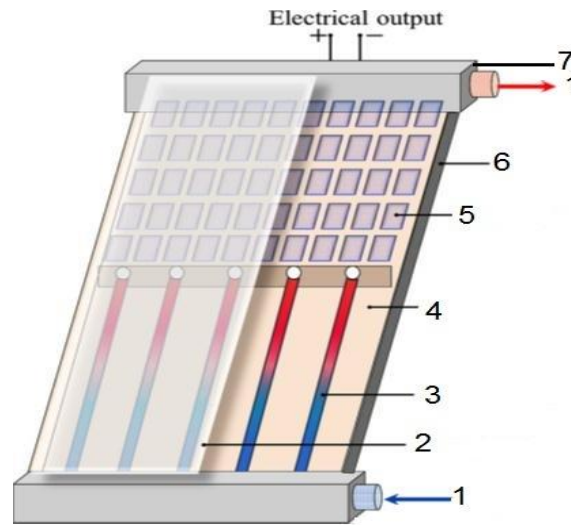


Fig. 1 Components of PV/T collector

Safari and Ataei did a thermal and electrical analysis of a linear parabolic concentrated photovoltaic/thermal hybrid solar collector. They investigated effect of different operational and design parameters on the electrical and thermal performances of this system (Safari and Ataei 2015).

Wongyu *et al.* (2016) did an experimental study of grid connected photovoltaic in cold climate region in US. They found in first year photovoltaic cells produced 5.801 kWh of AC electrical energy with 10.6% efficiency (Wongyu *et al.* 2016).

Carnevale *et al.* (2016) did a comparison of costs and environmental impacts of two renewable energy production technologies: wind turbine and photovoltaic cells. They used Eco-indicator's 95 method (Carnevale *et al.* 2016)

In the present research, since our goal is to optimize PV/T collectors for household applications, flat-plate PV/T collector with water as the cooling fluid was selected to be appropriate (because water has greater heat absorption capacity than air). Following thermal and electrical modeling of PV/T collector, the factors affecting this collector are optimized using genetic algorithm. The innovations and novelties of the research include:

- Preparation of a model that simultaneously considers thermal and electrical behaviors of the collector
- Optimization of selected parameter using genetic algorithm optimization procedure
- Utilization of the model for Iran's residential areas

2. System description

The collector under analysis consists of the following components:

1. Manifolds or headers for passing and discharging the heat-transmitting fluid, installed at the top and bottom of collector.
2. Plate protective glass
3. Tubes and channels for the flow of heat-transmitting fluid

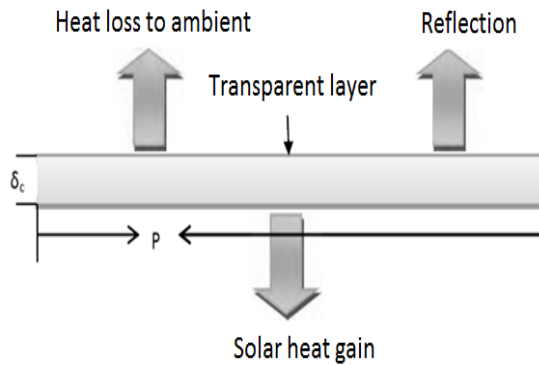


Fig. 2 Energy transfer paths in the transparent layer

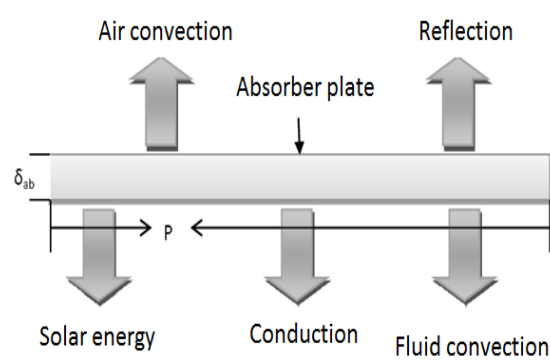


Fig. 3 Heat transfer paths from the transparent layer

Table 1 Corrections factors for climate types (Duffie and Beckman 1991)

Climate type	r_0	r_1	r_k
Tropical	0.95	0.98	1.02
Midlatitude summer	0.97	0.99	1.02
Subarctic summer	0.99	0.99	1.01
Midlatitude winter	1.03	1.01	1.00

4. Absorber plate
5. Photovoltaic plate
6. Equipment insulation that covers around and behind the collector and tubes for reducing heat dissipations.
7. Frame or transparent layer that embodies the collector parts and protects them against dust, moisture, and other external agents.

Conservation of energy equations shall be written in each component. As the solar energy enters the collector, some part of it is absorbed into the fluid (water flow), some amount is converted into electricity, some amount is dissipated to the ambient environment and the remainder is transferred to the earth or sky via radiation. Each of these cases can be visualized as a thermal resistance path. Thermal resistivity value of each aforementioned path is determined by evaluating conductive, convective, and radiation heat transfer coefficients. Figs. 2 and 3 respectively illustrate energy transfer paths in and from the transparent layer.

The clearance between transparent layer and absorber plate is air, where heat transfer is natural displacement which shall be derived from appropriate equations.

2.1 Radiation flux calculation

Extraterrestrial radiation flux incident on the plane normal to the radiation on the n^{th} day of the year and it is calculated by the following equation (Duffie and Beckman 1991)

$$G_{on}=G_{sc}(1.000110+0.034221 \cos B+0.001280 \sin B+0.000719 \cos 2B+0.000077 \sin 2B) \quad (2)$$

G_{sc} is a solar constant and it is equal to $1367 \text{ (W/m}^2\text{)}$ and n is a number of day ($n=1$ for 1st of January).

B is calculated by the following formula (Duffie and Beckman 1991)

$$B=(n-1) \frac{360}{365} \quad (3)$$

Total solar radiation on the tilted surface can be calculated by the following formula (Duffie and Beckman 1991)

$$G_T = G_b R_b + G_d \left(\frac{1+\cos\beta}{2} \right) + (G_b + G_d) \rho_g \left(\frac{1-\cos\beta}{2} \right) \quad (4)$$

In above equation, G_b is a beam radiation (W/m^2), G_d is a diffuse radiation (W/m^2), β is a title angle (degree), ρ_g is a solar reflectance from surroundings, ρ_g is diffuse reflectance constant and R_b is calculated by the following equation (Duffie and Beckman 1991)

$$R_b = \frac{\cos(\Phi-\beta) \cos\delta \cos\omega + \sin(\Phi-\beta) \sin\delta}{\cos\Phi \cos\delta \cos\omega + \sin\Phi \sin\delta} \quad (5)$$

In above equation Φ is a latitude angle, δ is a declination angle, ω is an hour angle.

Also, solar declination angle with respect to the equator is $(-23.45 \leq \delta \leq 23.45)$ (Duffie and Beckman 1991)

$$\delta = 23.45 \sin\left[360\left(\frac{284+n}{365}\right)\right] \quad (6)$$

Where, n is number of the day beginning from January 1st.

Beam radiation is calculated by the following equation (Duffie and Beckman 1991)

$$G_b = G_{on} \tau_b (\cos\Phi \cos\delta \cos\omega + \sin\Phi \sin\delta) \quad (7)$$

τ_b is a atmospheric transmittance for beam radiation,

τ_b is calculated by the following equation (Duffie and Beckman 1991)

$$\tau_b = a_0 + a_1 \cos\left(\frac{-k}{\cos\Phi \cos\delta \cos\omega + \sin\Phi \sin\delta}\right) \quad (8)$$

a_0 , a_1 and k are the variables of this equation and they are calculated by the following equations (Duffie and Beckman 1991)

$$a_0 = (0.4237 - 0.0082(6-A)^2) r_0 \quad (9)$$

$$a_1 = (0.5055 - 0.00595(6.5-A)^2) r_1 \quad (10)$$

$$k = (0.2711 + 0.1858(2.5-A)^2) r_k \quad (11)$$

A is altitude of the observer (km). Table 1 shows r_0 , r_1 and r_k for different climate types (Duffie and Beckman 1991).

2.2 Thermal analysis

At steady state, efficiency of a PV/T collector is described using energy balance which represents distribution of incidence solar energy into effective gained energy, thermal losses, and

optical losses. The solar radiation absorbed by a PV/T collector per unit area of absorber plate (S) equals the difference of solar radiation and optical losses. Heat losses to the ambient environment occur via conduction, convection, and radiation. For thermal analysis, the overall heat loss coefficient of collector shall be initially defined. Losses are divided into three parts: losses from top of collector (U_s), losses from back of the collector (U_b), and losses from the sides of collector (U_e) which are expressed as below (Duffie and Beckman 1991)

$$U_s = \left(\frac{N}{\frac{C}{T_{cm}} \left[\frac{T_{cm} - T_{amb}}{N + f} \right]^e + \frac{1}{h_w}} \right)^{-1} + \frac{\sigma(T_{cm} + T_{amb})(T_{cm}^2 + T_{amb}^2)}{\frac{1}{\tau_c + 0.00591 N h_w} + \frac{2N + f - 1 + 0.133 \epsilon_c - N}{\tau_g}} \quad (12)$$

$$f = (1 + 0.089h_w - 0.1166h_w\tau_c)(1 + 0.07866N) \quad (13)$$

$$C = 520(1 - 0.000051\beta^2) \quad (14)$$

$$e = 0.430 \left(1 - \frac{100}{T_{cm}} \right) \quad (15)$$

Where, N is number of glass covers (transparent layers), β is collector inclination (degrees), τ_g is glass diffusivity, τ_c is cell diffusivity, T_{amb} is the ambient temperature (K), T_{cm} is average cell temperature (K), h_w is wind heat transfer coefficient (W/m^2K). Heat loss coefficient from back of collector approximately is (Duffie and Beckman 1991)

$$U_b = \frac{1}{R_3 + R_4} = \frac{k_h}{L_h} + \frac{k_{ins}}{L_{ins}} \quad (16)$$

k_h is thermal conductivity of absorber plate (W/mK), k_{ins} is thermal conductivity of insulator ($W/m K$), L_h is thickness of absorber plate (m) and L_{ins} is thickness of insulator (m).

Losses from the sides of the collector system are estimated with the assumption of one-dimensional lateral heat flow around the collector system. These losses are estimated as follows (Duffie and Beckman 1991)

$$U_e = \frac{(UA)_{edge}}{A_c} \quad (17)$$

In the equation above, U is loss coefficient of corner (W/m^2K), A is surface area of collector side (m^2), and A_c is surface area of the collector (m^2). Accordingly, total heat loss of the system will be equal to (Duffie and Beckman 1991)

$$U_L = U_s + U_b + U_e \quad (18)$$

Energy balance for the glass (transparent layer), PV module, and absorber plate (Kroib *et al.* 2014)

$$\tau_g[\alpha_{cell}\beta_{cell}G + \alpha_T(1 - \beta_{cell})G]Db = [U_t(T_{cell} - T_{amb}) + U_T(T_{cell} - T_{bs})] \times Db + \tau_g\beta_{cell}\eta_{el}GD \quad (19)$$

In the equation above, T_{cell} : temperature of photovoltaic cell (K), T_{amb} : ambient temperature (K), T_{bs} : temperature of absorber plate (K), G : solar radiation intensity (W/m^2), D : width of absorber plate on the flow line (m), b : length of the flow line (m), α_{cell} : absorption coefficient of

photovoltaic cell, α_T : absorption coefficient of absorber layer, β_{cell} : compressibility of photovoltaic cell, τ_g : diffusivity of glass cover, U_T : total heat transfer coefficient of PV cell to absorber plate ($\text{W}/\text{m}^2\text{K}$), U_t : total heat transfer coefficient of PV cell to ambient environment ($\text{W}/\text{m}^2\text{K}$), and η_{el} : electrical efficiency of photovoltaic module.

Rate of heat transfer to the absorber plate is calculated by the following equation (Kroib *et al.* 2014)

$$(\alpha\tau)_{eff} G_T = (T_{cell} - T_{bs})U_T + (T_{cell} - T_{amb})U_t \quad (20)$$

Where, $(\alpha\tau)_{eff}$ is product of effective absorption and transfer, expressed as below (Sobhnamayan *et al.* 2014)

$$(\alpha\tau)_{eff} = \tau_g[\alpha_{cell} \beta_{cell} + \alpha_T(1 - \beta_{cell}) - \beta_{cell}\eta_{el}] \quad (21)$$

Temperature of photovoltaic cell can be obtained from the following equation (Kroib *et al.* 2014)

$$T_{cell} = \left[\frac{(\alpha\tau)_{eff} G + T_{amb} U_t + T_{bs} U_T}{U_t + U_T} \right] \quad (22)$$

Energy balance for the absorber layer is (Kroib *et al.* 2014)

$$U_T(T_{cell} - T_{bs})Db = h_f(T_{bs} - T_f)Db \quad (23)$$

From which, temperature of absorber layer can be determined as below (Kroib *et al.* 2014)

$$T_{bs} = \frac{h_{p1} (\alpha\tau)_{eff} G + U_{tT} T_{amb} + h_f T_f}{U_{tT} + h_f} \quad (24)$$

In this equation, h_f is heat transfer coefficient inside the flow path ($\text{W}/\text{m}^2\text{K}$), h_{p1} is punishment coefficient due to presence of photovoltaic cell materials and cell in the PV module, T_f is average temperature of fluid (K), and U_{tT} is total heat transfer coefficient between the upper level and absorber plate ($\text{W}/\text{m}^2\text{K}$). Energy balance for the fluid in the flow path (Kroib *et al.* 2014)

$$\frac{\dot{m}}{M} C_p T_f|_{x+dx} - \frac{\dot{m}}{M} C_p T_f|_x - \frac{1}{M} d\dot{Q}_u dx = 0 \quad (25)$$

$$\left\{ \begin{array}{l} \frac{dT_f}{dx} + \left(\frac{W F' U_L}{\dot{m} C_p / M} \right) (T_f - T_{amb}) = \frac{W F' h_{p1} h_{p2} (\alpha\tau)_{eff} G}{\dot{m} C_p / M} \\ x = 0 \rightarrow T_f = T_{f,in} \end{array} \right. \quad (26)$$

According to above equation, average fluid temperature can be evaluated via integration (Duffie and Beckman 1991)

$$T_{fm} = \frac{1}{L} \int_0^L T_f(y) dy \quad (27)$$

Via integrating and substituting F_R and Q_U in the former equation, average fluid temperature is derived as (Duffie and Beckman 1991)

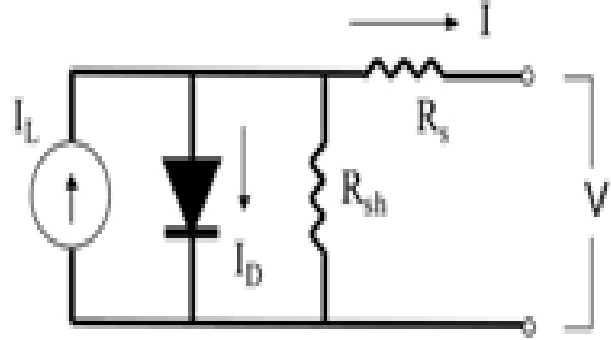


Fig. 4 Equivalent circuit for photovoltaic cell

$$T_{fm} = T_{fi} + \frac{Q_u/A_c}{F_R U_L} (1 - F''). \quad (28)$$

That can be also written as (Duffie and Beckman 1991)

$$T_{fm} = \left[\frac{h_{p1} h_{p2} (\alpha\tau)_{eff} G}{U_L} + T_{amb} \right] \left[1 + \frac{1 - \exp\left(-\frac{A_c F' U_L}{\dot{m} C_p}\right)}{\frac{A_c F' U_L}{\dot{m} C_p}} \right] + T_{fi} \left(\frac{1 - \exp\left(-\frac{A_c F' U_L}{\dot{m} C_p}\right)}{\frac{A_c F' U_L}{\dot{m} C_p}} \right) \quad (29)$$

Where, U_L is total heat loss coefficient (W/m^2K), W is space between two adjacent flow lines (m), M is the number of flow lines, F' is efficiency or output coefficient of collector, and h_{p2} is punishment coefficient due to presence of tedlar between the fluid and surface of photovoltaic module, and $A_c = bL$ where b is length of flow line (m) and $L = MW$ in meters. Outlet water temperature of PV/T collector is expressed as below (Kroib *et al.* 2014)

$$T_{f,out} = T_{f,in} \exp\left(-\frac{F' U_L A_c}{\dot{m} C_p}\right) + \left(T_{amb} + \frac{h_{p1} h_{p2} (\alpha\tau)_{eff} G}{U_L} \right) \left[1 - \exp\left(-\frac{F' U_L A_c}{\dot{m} C_p}\right) \right] \quad (30)$$

Maximum possible effective energy gain (heat transfer) in a PV/T collector happens when collector is at the same temperature as inlet fluid because heat losses to the ambient environment would be minimum. Balance of this energy is expressed as follows, which incorporates maximum effective energy gain from the collector (Duffie and Beckman 1991)

$$Q_u = F_R A_c \left[h_{p1} h_{p2} (\alpha\tau)_{eff} G - U_L (T_{f,in} - T_{amb}) \right]. \quad (31)$$

Thermal efficiency of PV/T collectors is expressed as (Duffie and Beckman 1991)

$$\eta_{th} = \frac{Q_u}{A_c G} \quad (32)$$

According to the collector under analysis and the calculated energy balance, the equation can be rewritten as (Duffie and Beckman 1991)

$$\eta_{th} = F_R \left[h_{p1} h_{p2} (\alpha\tau)_{eff} - \frac{U_L (T_{f,in} - T_{amb})}{G} \right] \quad (33)$$

2.3 Electrical analysis

In order to compute the electrical parameters and electrical efficiency, a 4-parameter model for characteristic electrical current-voltage (V-I) curve of photovoltaic module is proposed based on the equivalent circuit shown in Fig. 4 (Sobhnamayan 2014)

$$I = I_L - I_0 \left[\exp\left(\frac{V + IR_s}{a}\right) - 1 \right] - \frac{V + IR_s}{R_{sh}} \quad (34)$$

Solving the model with the aid of following boundary conditions, five parameters were acquired namely “ a ” utility coefficient (V), I_L electrical current intensity of light (A), I_0 reverse saturation current of diode (A), and R_s series resistance (Ω). In the equation above, utility coefficient (a) is derived as below (Sobhnamayan *et al.* 2014)

$$a = \frac{n K T N_s}{q} \quad (35)$$

Where, n is an ideality factor, K is Boltzmann constant ($1.381 \times 10^{-23} \text{J/K}$), T is cell temperature (K), N_s number of cells in series, and q is the electrical charge (1.602×10^{-19} Colombes). To determine four parameters at reference conditions, one requires four boundary conditions of short-circuit current ($I=I_{sc,ref}$, $V=0$), open circuit voltage ($I=0$, $V=V_{oc,ref}$), and point of maximum power ($I=I_{mp,ref}$, $V=V_{mp,ref}$, $[d(IV)/dV]_{mp}=0$). Via substitution of these conditions in Eq. (25), a non-linear system will be obtained with 4 equations and 4 unknowns. The simplified equations are written below (Sobhnamayan *et al.* 2014)

$$I \approx I_{L,ref} - I_{o,ref} \left[\exp\left(\frac{V + I_{sc,ref} R_{s,ref}}{a_{ref}}\right) \right] \quad (36)$$

$$0 \approx I_{sc,ref} + I_{L,ref} \quad (37)$$

$$0 = I_{L,ref} - I_{o,ref} \left[\exp\left(\frac{V_{oc,ref}}{a_{ref}}\right) \right] \quad (38)$$

$$0 \approx -I_{mp,ref} + I_{L,ref} - I_{o,ref} \left[\exp\left(\frac{V_{mp,ref} + I_{mp,ref} R_{s,ref}}{a_{ref}}\right) \right] \quad (39)$$

The subscript (*ref*) denotes parameter at reference conditions in which solar radiation intensity is $G_{ref}=1000 \text{W/m}^2$ and cell temperature equals $T_{cell,ref}=25^\circ\text{C}$ and a spectral distribution corresponding to air mass of 1.5. Solving the simplified form of equation system above for reference parameters yields the following equations (Sobhnamayan *et al.* 2014)

$$I_{L,ref} = I_{sc,ref} \quad (40)$$

$$I_{o,ref} = \frac{I_{sc,ref}}{\exp(V_{oc,ref}/a_{ref})} \quad (41)$$

$$R_{s,ref} = \frac{a_{ref} \ln\left(1 - \frac{I_{mp,ref}}{I_{sc,ref}}\right) + V_{oc,ref} - V_{mp,ref}}{I_{mp,ref}} \quad (42)$$

$$a_{ref} = \frac{2V_{mp,ref} - V_{oc,ref}}{\frac{I_{mp,ref}}{I_{sc,ref} - I_{mp,ref}} + \ln\left(1 - \frac{I_{mp,ref}}{I_{sc,ref}}\right)} \quad (43)$$

Values of $V_{oc,ref}$, $I_{sc,ref}$, $V_{mp,ref}$ and $I_{mp,ref}$ at reference conditions are normally provided by manufacturers of the photovoltaic modules. To evaluate voltage and electrical current intensity and other model parameters at new operational conditions, series of transfer equations are used as below (Sobhnamayan *et al.* 2014)

$$\frac{a}{a_{ref}} = \frac{T_{cell}}{T_{cell,ref}} \quad (44)$$

$$I_L = \frac{S}{S_{ref}} [I_{L,ref} + \mu_{I,sc}(T_{cell} - T_{cell,ref})] \quad (45)$$

$$\frac{I_o}{I_{o,ref}} = \left(\frac{T_{cell}}{T_{cell,ref}}\right)^3 \exp\left(\frac{EN_c}{a_{ref}}\left(1 - \frac{T_{cell,ref}}{T_{cell}}\right)\right) \quad (46)$$

$$\Delta T = T_{cell} - T_{cell,ref} \quad (47)$$

$$\Delta I = \mu_{I,sc}\left(\frac{S}{S_{ref}}\right)\Delta T + \left(\frac{S}{S_{ref}} - 1\right)I_{sc,ref} \quad (48)$$

$$\Delta V = \mu_{V,oc}\Delta T - R_s\Delta I \quad (49)$$

$$I_{sc,new} = I_{sc,ref} + \Delta I \quad (50)$$

$$V_{oc,new} = V_{oc,ref} + \Delta V \quad (51)$$

$$\frac{R_{sh}}{R_{sh,ref}} = \frac{S_{ref}}{S} \quad (52)$$

Where, E is a semiconductor's band gap energy (J), N_c is a number photovoltaic cells in series, $\mu_{I,sc}$ is a temperature coefficient of electrical current (A/K), and $\mu_{v,oc}$: temperature coefficient of voltage (V/K). Also, for finding maximal power, the equation $P=VI$ is differentiated with respect to V and is then set equal to zero, which ultimately gives (Duffie and Beckman 1991)

$$\frac{I_{mp}}{V_{mp}} = \left[\frac{\frac{I_o}{a} \exp\left(\frac{V_{mp} + I_{mp}R_s}{a}\right) + \frac{1}{R_{sh}}}{1 + \frac{R_s}{R_{sh}} + \frac{I_o R_s}{a} \exp\left(\frac{V_{mp} + I_{mp}R_s}{a}\right)} \right] \quad (53)$$

General form of V-I equation at point of maximum power is (Duffie and Beckman 1991)

$$I_{mp} = I_L - I_o \left[\exp\left(\frac{V_{mp} + I_{mp}R_s}{a}\right) - 1 \right] - \frac{V_{mp} + I_{mp}R_s}{R_{sh}} \quad (54)$$

Table 2 Values related to the collector under analysis

1	Collector length	2000 mm
2	Collector width	1000 mm
3	Diameter of water tube	10 mm
4	Step of tubes	150 mm
5	Transmissibility of transparent layer	0.85
6	Thermal conductivity of insulator	0.035 W/mK

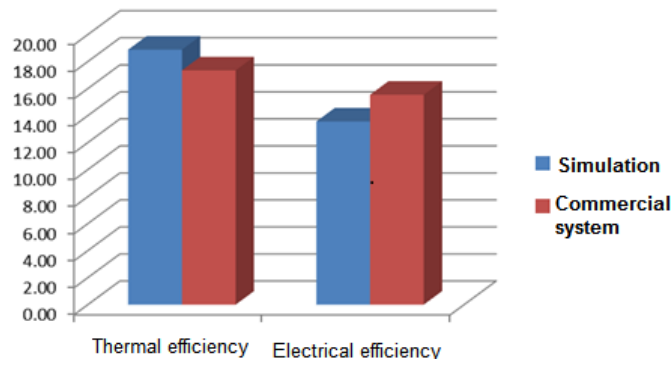


Fig. 5 Comparison of thermal-electrical efficiency from simulation and manufacturer data

Potential difference and electrical current intensity at point of maximum power can be derived by simultaneously solving Eqs. (54) and (55). Now, the maximum power of photovoltaic cell can be expressed as follows (Duffie and Beckman 1991)

$$\eta_{mp} = \frac{I_{mp} V_{mp}}{A_{PV/T} G_T} \quad (55)$$

Taking into account the fact that part of the generated electrical energy shall be used for pump operation, the electrical efficiency of PV/T collector is finally derived as (Sobhnamayan *et al.* 2014)

$$\eta_{el} = \frac{I_{mp} V_{mp} - P_{pump}}{A_{PV/T} G_T} \quad (56)$$

Having the thermal and electrical efficiencies of PV/T collector, total efficiency of system can be now evaluated (Sobhnamayan *et al.* 2014) and (Al-Saadi 2014)

$$\eta_{oV} = \eta_{th} + \eta_{el}/0.38 \quad (57)$$

Thermal and electrical energies do not have the same quality. Thus, a multiplier equal to 0.38 is assigned in Eq. (57) for converting electrical energy into its equivalent heat.

3. Results and discussion

By using the following equations, photovoltaic hybrid collector was modeled. To evaluation of

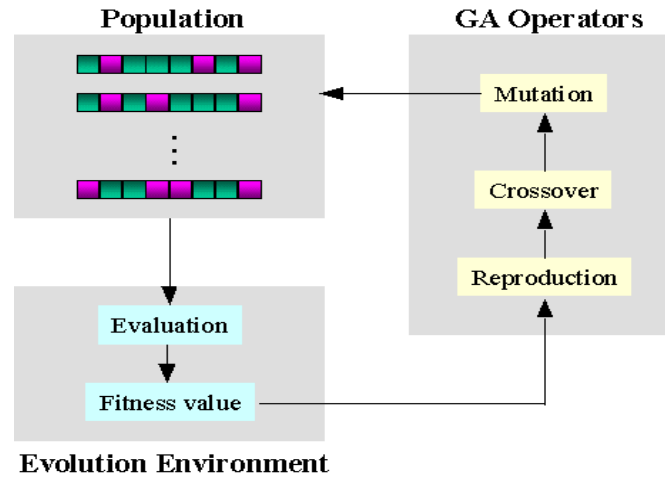


Fig. 6 Evolution process in genetic algorithm (Mostafa 2012)

results, data calculated from the model was compared by the data calculated from the model. The values in Table 1 have been roughly extracted from design information of a manufacturing company in order to enable data validation (www.tessolarwater.com).

Average collector efficiency at steady state is compared with manufacturer data of commercial collector equipment. The acquired results are illustrated in Fig. 5. The comparison indicated that the two sets of data are to a large extent similar.

The main idea behind evolutionary algorithms was introduced by Rechenberg in 1960 (Holland 1992). Genetic algorithms, including branches of these types of algorithms, are computer search methods based on optimizing algorithms and gene and chromosome structures; they were introduced to Holland at Michigan University and developed by students like Goldenberg (Goldberg 1989), (Srinivas and Deb 1994). The general idea of the multi-objective non-dominated sorting genetic algorithm (NSGA) was introduced by Goldenberg in 1989 and then implemented by Deb and Srinvas (Deb *et al.* 2000). An extension of the NSGA algorithm, NSGAI, was proposed by Deb *et al.* (Deb *et al.* 2000). In NSGAI, some solutions for each generation are chosen by the Binary Tournament Selection method. At the first rating, the criterion for selection of a solution is the solution's ranking, and at the second rating, this criterion relates to crowding distance regarding the solution. The lower is the solution ranking and the greater is the crowding distance, the more favorable is the solution.

By repeating the selection of the operator on the population of every generation, a combination of individuals of that generation is chosen to take part in crossover and mutation. The act of crossover occurs on some parts of the set of selected people and the act of mutation is applied on the remaining parts, and this leads to the creation of a child population and mutants, which are merged with the main population. First, members of the created population are sorted in ranking and ascending order. Members of the population with the same rank are sorted on the basis of crowding distance and descending order. At this point, members of the population have been sorted firstly by rank and secondly by crowding distance. The main members of the population are selected from the top of the list equal to the people of the main population and the rest are set aside. The chosen members produce the population of the next generation and this cycle is repeated until the concluding conditions are reached (Deb *et al.* 2000). Fig. 6 illustrates evolution

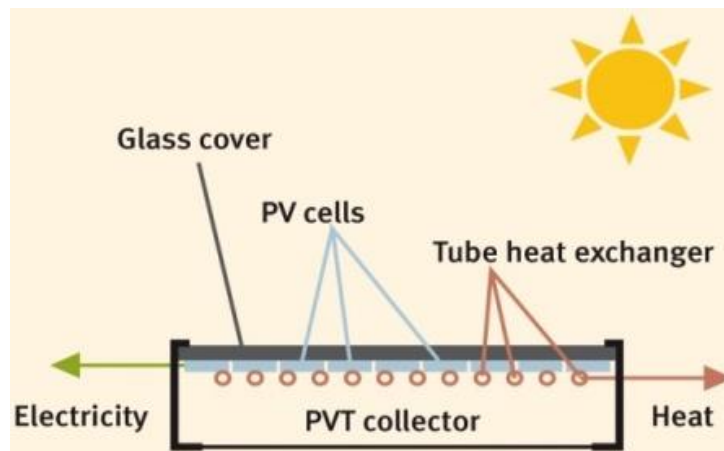


Fig. 7 Schematic diagram of the collector under study

process in genetic algorithm (Mostafa 2012).

Genetic algorithm has been highly successful for classical optimization methods in solving linear and convex problems and some analogous situations but this method proves by far more efficient in solving discrete and non-linear problems. In nature, better generations emerge via combination of fitter chromosomes. Meanwhile some mutations occur in chromosomes as well that might lead to improvement of subsequent generations. Genetic algorithm also solves the problems using this idea. There exists a remarkable difference between genetic algorithm and most conventional search and optimization techniques. The 4 major differences include:

1. Genetic algorithm simultaneously searches a set of point and not a single point.
2. Genetic algorithm obeys probabilistic rules and not natural laws.
3. Genetic algorithm acts on a set of encoded properties and not on their principal values (except in cases for which actual representation of strings is used).
4. Genetic algorithm does not need differentiation and/or any sort of supplementary information and only objective function and fitness determination method of raw data mandate the search direction.

The important point is that genetic algorithm provides a series of potential responses and the final solution is selected by the user. In cases where the problem lacks a unique solution, such as multi-objective optimization, genetic algorithm is helpful for simultaneous determination of solutions.

The modeled equipment comprises a hybrid flat-plate collector (PV/T). A transparent layer (glass cover) lies on the collector and a photovoltaic cell absorbs the radiated sunlight, some part of the energy is converted into electricity and the rest is used for heating the water flowing in the tubes beneath the absorber plate. The following items further highlight significance of the study:

- Electrical efficiency of absorber plate is a function of temperature. Higher temperature of the plate will lower the efficiency of photovoltaic cell.
- On the other hand, electrical energy is more valuable than thermal energy.

Consequently, the assumption is that a range of parameters can be found at one or several points such that total efficiency of the system (sum of thermal and electrical efficiencies with proper conversion factor) would be improved via enhancing heat recovery from the system, and hence, reducing temperature of collector plate.

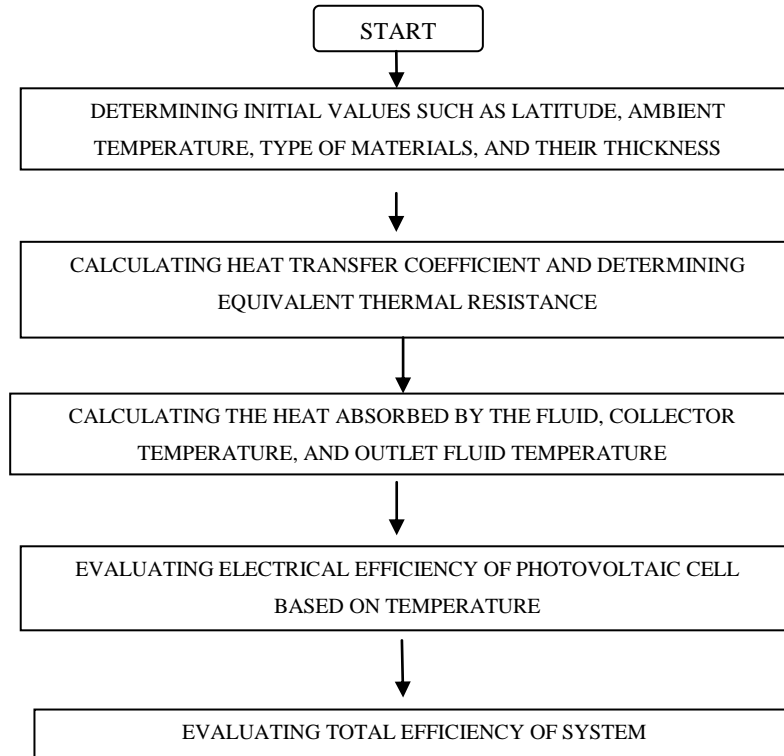


Fig. 8 Flowchart of solution algorithm

Following thermal and electrical modeling of system in a computer program, the subsequent step is optimization of the parameters affecting the performance. To do so, some criterion needs to be introduced to evaluate the system performance. This criterion is referred to as “objective function”. Like any energy generating machine, it is advisable to choose energy efficiency (Eq. (48)) as the objective function. As genetic algorithm method tends to minimize the value of objective function, so objective function due to physical restrictions are defined as below, it is noticeable that minimizing the following equation is appropriate for us

$$F = 1 - (\eta_{thermal} + (\eta_{elec}/.38)) \quad (58)$$

A conversion factor was applied to unify of electrical and thermal efficiencies. Since values of these two types of energies do not have the same quality. Thus, a 0.38 multiplier is assigned for electrical efficiency for converting electrical energy into its equivalent heat (Sobhnamayan 2014), (Al-Saadi 2014). By this defined objective function, total efficiency of hybrid photovoltaic system can be optimized.

Optimization parameters include fluid flow rate and collector inclination angle. Variation intervals of the respective parameters in optimization are included in Eq. (59)

$$\begin{aligned} 0.25 &\leq \text{water flow rate (gpm)} \leq 5 \\ 20 &\leq \text{Collector angle } (^{\circ}) \leq 70. \end{aligned} \quad (59)$$

Table 3 Geographical conditions of Tehran (Province of Iran)

Parameters	Value	
Latitude	35°	
Longitude	51°	
Average wind speed	1.5 m/s	
Average weather fairness coefficient	1	
Ambient air temperature in different months	Jan	8.5
	Feb	10.5
	Mar	16.4
	Apr	16.9
	May	27.4
	Jun	30.8
	Jul	32.5
	Aug	32.5
	Sep	29.6
	Oct	23.6
	Nov	13.5
	Dec	11.4

Table 4 Collector specifications

Parameters	Value
Collector length	2000 mm
Collector width	1000 mm
Step of tubes	150 mm
Diameter of tubes	12.5 mm
Material type of photovoltaic module	Polycrystalline
Material type of absorber plate	Copper
Material type of tubes	Copper
Material type of transparent layer	Glass
Transmissibility of transparent layer	0.85

Domains of the optimization parameters including fluid flow rate and collector inclination angle were determined with the aid of engineering experience and optimal values were sought for in these domains using genetic algorithm. Some parameters were assumed as constant like latitude $\theta=35$, diameter of tubes $d=12.5$ mm, step of tubes $p=150$ mm, and wind speed $V=1.5$ m/s. The respective values either depend on the location such as latitude and wind speed or are standard industrial values such as step and diameter of tubes. General procedure of solution and flowchart of solution algorithm are shown in Fig. 8.

Of course, the above solution algorithm does not show genetic method. Genetic algorithm was used in MATLAB software. Tables 3 and 4 include geographical conditions of Tehran (Province of Iran) as sample and collector specifications:

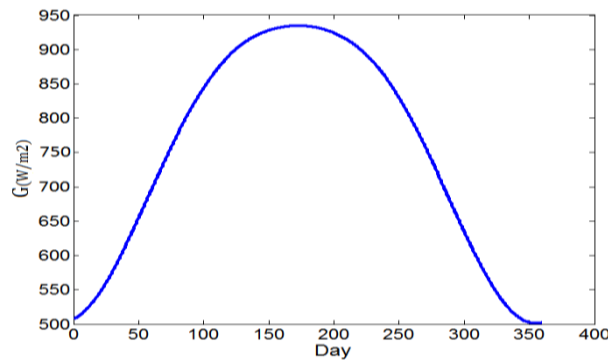


Fig. 9 Solar radiation during the year in Tehran (province of Iran)

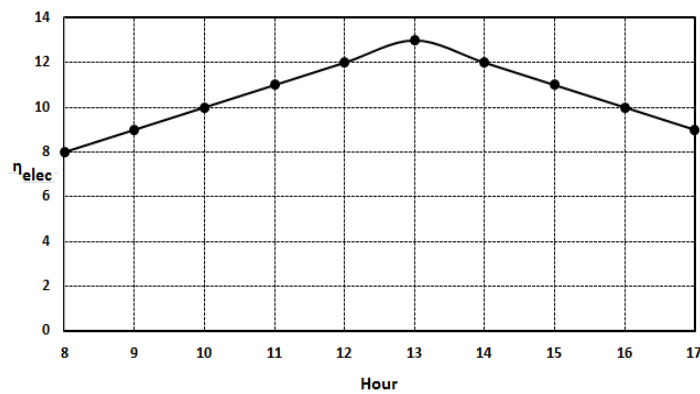


Fig. 10 Electrical efficiency for a collector at an angle of 45 degrees, with water flow rate of 2 gallons per minute. Location of system is in Tehran (province of Iran) in February

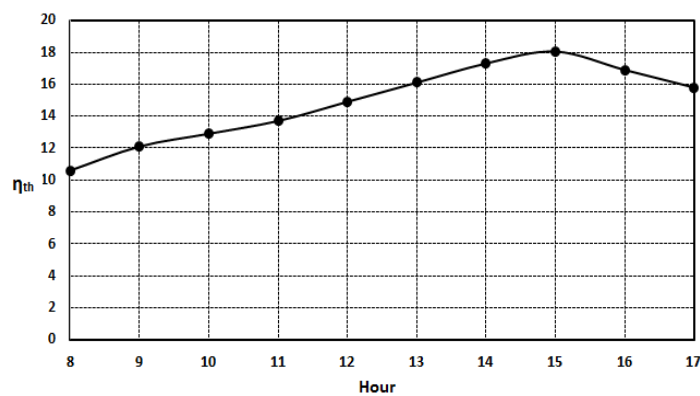


Fig. 11 Thermal efficiency for a collector at an angle of 45 degrees, with water flow rate of 2 gallons per minute. Location of system is in Tehran (province of Iran) in February

Total solar radiation was calculated in different days of the year based on solar declination angle. Fig. 9 represents solar radiation curve during the year.

Figs. 10, 11 and 12 illustrate electrical, thermal and total efficiencies for a collector at an angle of 45 degrees, with water flow rate of 2 gallons per minute. Location of system is in Tehran

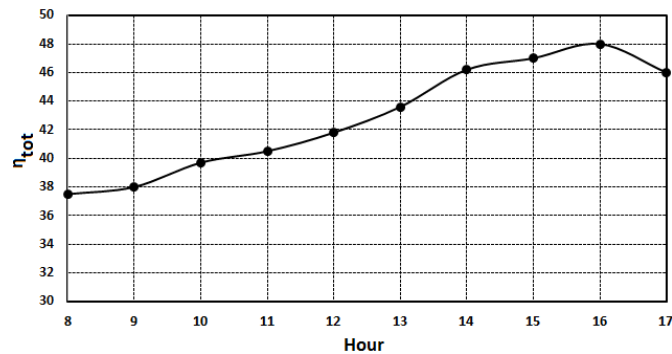


Fig. 12 Total efficiency for a collector at an angle of 45 degrees, with water flow rate of 2 gallons per minute. Location of system is in Tehran (province of Iran) in February

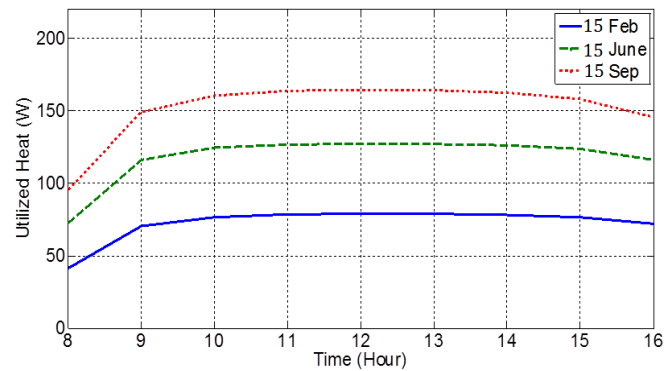


Fig. 13 The heat absorbed by the collector in three specific days of the year in the 15th day of February, June, and September

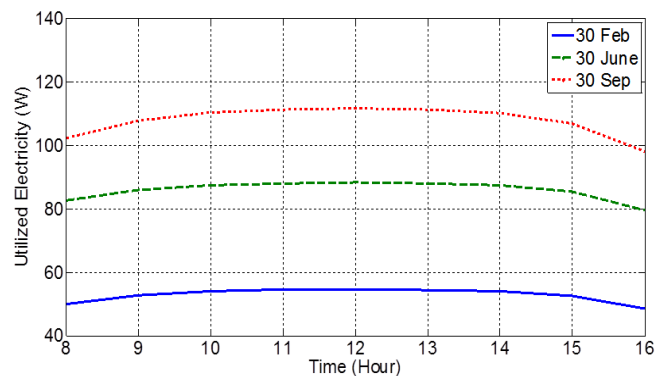


Fig. 14 The electricity absorbed by the collector in three specific days of the year in the 15th day of February, June, and September

(province of Iran) in February. The reason for using gallon/min as the flow rate unit is its easier comprehension for the people working in constructional installations industry.

Amounts of the heat and electricity absorbed and generated by the collector in the 15th day of February, June, and September are respectively shown in Figs. 13 and 14.

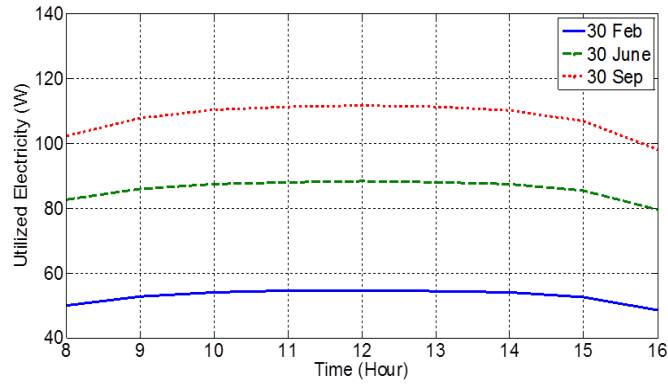


Fig. 14 The electricity absorbed by the collector in three specific days of the year in the 15th day of February, June, and September

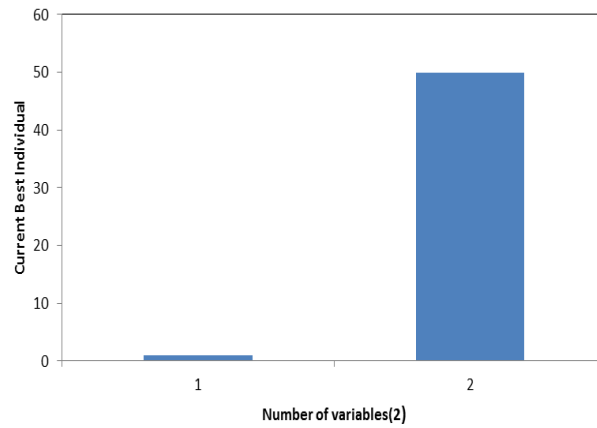


Fig. 15 Optimal values of parameters

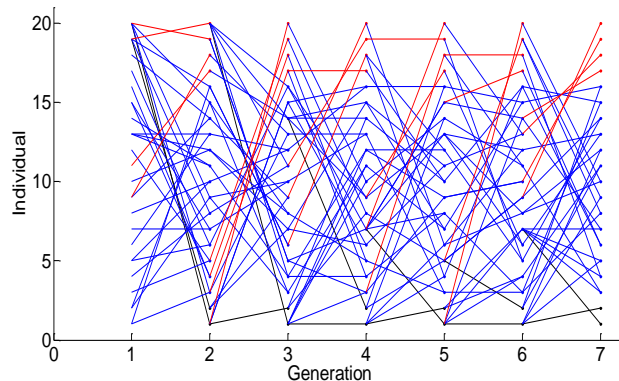


Fig. 16 Evolution mechanism of parameter selection

As seen in Fig. 13, thermal energy value is minimal during early hours of sunrise. The reason is thermal inertia of the equipment Thermal energy is increased by the course of time until reaching to the stable value. Fig. 14 illustrates this trend for thermal efficiency. Similarly, Fig. 12 manifests

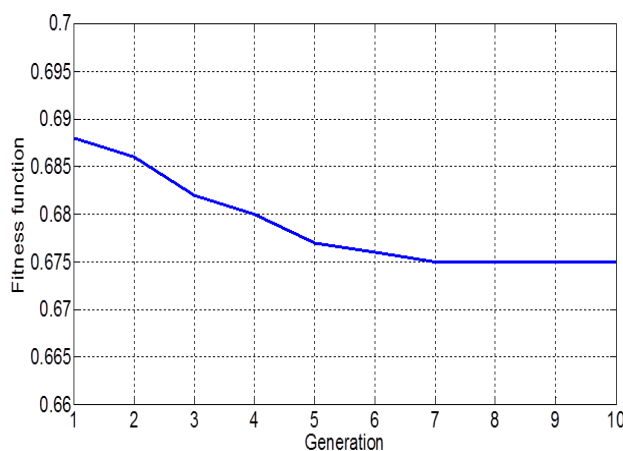


Fig. 17 Value of objective function in different generations

Table 5 Values of generated thermal and electrical energies in specific days of the year (Location: Tehran)

15 th day of month	Average amount of generated heat (W)		Average amount of generated electricity (W)	
	Non-optimal case (%)	Optimal case (%)	Non-optimal case (%)	Optimal case (%)
Jan	91.3	97	69.7	71.9
Feb	110.9	118.3	82.3	85.2
Mar	131	140.5	94.1	97.7
Apr	145.6	155.4	101.9	106.1
May	153.1	162.1	105.3	109.8
Jun	154.3	162.9	105.8	110.4
Jul	150.1	159.9	104.1	108.4
Aug	138.9	149	98.7	102.6
Sep	121.8	130.5	88.7	91.9
Oct	100.6	107.3	75.9	78.4
Nov	84.4	89.5	64.9	66.9
Dec	79.5	84.4	61.6	63.4

that small amount of electrical energy is generated during initial hours of operation when collector and ambient air have the same temperature and also because solar energy is weak in the early morning. However, value of electrical efficiency is maximum according to Fig. 14. Electrical efficiency declines with heating the collector and temperature rise of photovoltaic plate. As expected, the lowest and highest levels of energy are acquired in summer and winter, respectively.

Optimal values for the parameters under analysis are demonstrated in Fig. 15. As clearly observed, flow rate of approximately 1 (gpm) is the best value. Furthermore, the optimal angle is around 50 degrees. This result is completely in accordance with the rule of thumb that suggests collector angle shall be slightly greater than latitude. It must be also noted that angle is input as radians in computer simulations.

Procedures of growth and evolution of selections in genetic algorithm are illustrated in Fig. 16.

As shown in the diagram of Fig. 17, from the 7th generation onward, value of objective function

Table 6 Electrical, thermal and total efficiencies in specific days of the year (Location: Tehran)

15 th day of month	Thermal efficiency (%)		Electrical efficiency (%)		Total efficiency (%)	
	Non-optimal case (%)	Optimal case (%)	Non-optimal case (%)	Optimal case (%)	Non-optimal case (%)	Optimal case (%)
Jan	16.2	17.2	12.5	12.9	49.1	51.2
Feb	16.3	17.4	12.2	12.7	48.51	50.8
Mar	16.5	17.7	12	12.4	48.1	50.5
Apr	16.7	17.8	11.8	12.3	47.91	50.3
May	16.9	17.9	11.8	12.3	47.91	50.2
Jun	17	17.9	11.7	12.2	47.9	50.2
Jul	16.8	17.9	11.8	12.3	47.9	50.3
Aug	16.6	17.8	11.9	12.4	47.9	50.4
Sep	16.5	17.6	12.1	12.5	48.3	50.7
Oct	16.2	17.3	12.4	12.8	48.8	51
Nov	16.2	17.2	12.6	13.0	49.4	51.4
Dec	16.2	17.2	12.7	13.1	49.5	51.6

Table 7 Efficiency improvement percentages in the specific days of the year (Location: Tehran)

15 th day of month	Thermal efficiency		Electrical efficiency		Total efficiency	
	Improvement compared to non-optimal case (%)	Optimal case (%)	Improvement compared to non-optimal case (%)	Optimal case (%)	Improvement compared to non-optimal case (%)	Optimal case (%)
Jan	6.3	17.2	3.2	12.9	4.3	51.2
Feb	6.7	17.4	3.5	12.6	4.6	50.8
Mar	7.2	17.7	3.8	12.4	5.1	50.5
Apr	6.8	17.9	4.1	12.3	5.1	50.3
May	5.8	17.9	4.3	12.3	4.9	50.2
Jun	5.6	17.9	4.3	12.2	4.8	50.2
Jul	6.5	17.9	4.2	12.3	5.1	50.3
Aug	7.3	17.8	4	12.4	5.2	50.4
Sep	7.1	17.6	3.6	12.5	4.9	50.7
Oct	6.7	17.3	3.3	12.8	4.5	51.2
Nov	6	17.2	3.1	13.0	4.1	51.4
Dec	6.2	17.2	3	13.1	4.1	51.6

becomes nearly constant or converges in other words.

Also, values of generated thermal and electrical energies as well as electrical, thermal, and total efficiencies in specific days of the year (Location: Tehran) are included in Tables 5 and 6.

Also, improvement percentages of efficiency are included in Table 7.

As observed, with selection of optimal values, thermal and electrical efficiencies respectively improve by 6% and 3% while total efficiency improves by 5%. This optimized values is compared by selected data in reference 22, total annual error is about 5%. The improvement percentage

might seem not so impressive but it shall be reminded that the improvement levels are obtained for selecting the values at standard domains and improvement will be larger if the parameters are chosen beyond the domain. Additionally, no extra investment is needed for achieving these levels of improvement and they are achievable merely by adjusting the operational parameters.

4. Conclusions

PV/T solar collector with water as the cooling fluid was modeled in the current study. After modeling and model validation, major parameters including collector inclination angle and water flow rate were optimized. The analyses were performed in three specific days: 15th day of February, June, and September. Optimization was carried out using genetic algorithm method and aimed at reaching to the highest value of total thermal and electrical efficiencies. It was found out in the results that the amount of energy generated by the collector can be improved by selecting the operational parameters of hybrid collector including fluid flow rate and inclination angle. Annual improvement percentage during the initial moments is considerable and nearly equal to 17% when this system is located in Tehran. The reason is low temperature of collector during early times and temperature dependence of collector's thermal efficiency. Although improvement level at steady state is not like the initial times, the total energy absorption will be enhanced around 5% during the whole year. This enhancement can be achieved without imposing any additional expenditure. For future studies, hourly temperature of the environment from the Meteorology Organization can be added to the model. Furthermore, selection of synthetic oils as a working fluid is appropriate for the study. Among the advantages of this optimization are reduction of environmental contamination, reduced reliance on electricity lines and fossil fuels, mitigation of system repair and maintenance, and decrease in the required space. One disadvantage of the method also includes high initial expense of the system; nonetheless, a reduction in costs is predicted due to progress trend of this technology and its prevalence all over the world.

References

- Agrawal, S. and Tiwari, G.N. (2011), "Energy and exergy analysis of hybrid micro-channel photovoltaic thermal module", *Sol. Energy*, **86**(2), 356-370.
- Aleklett, K., Höök, M., Jakobson, K., Lardelli, M., Snowden, S. and Söderbergh, B. (2010), "The peak of the oil age-analyzing the world oil production reference scenario in world energy outlook 2008", *Energy Pol.*, **38**(3), 1398-1414.
- Al-Saadi, H., Al-Sayed, R., Al-Sheikh, M. and Al-Bahadili, H. (2014), "Simulation of maximum power point tracking for photovoltaic systems", *Energy Pow. Eng.*, **8**, 741-748.
- Aste, N., Pero, C. and Leonforte, F. (2014), "Water flat plate PV-thermal collectors", *Sol. Energy*, **102**, 98-115.
- Bakar, M.N.A., Othman, M., Din, M.N., Manaf, N.A. and Jarimi, H. (2014), "Design concept and mathematical model of a bi-fluid photovoltaic/thermal (PV/T) solar collector", *Renew. Energy*, **4**, 1-12.
- Carnevale, E.A., Lidia Lombardi, L. and Zanchi, L. (2016), "Wind and solar energy: A comparison of costs and environmental impacts", *Adv. Energy Res.*, **4**(2), 21-146.
- Choi, W., Warren, R.D. and Pate, M.B. (2016), "An experimental performance analysis of a cold region stationary photovoltaic system", *Adv. Energy Res.*, **4**(1), 1-28.
- Deb, K., Agrawal, S., Pratab, A. and Meyarivan, T. (2000), "A fast elitist none-dominated sorting in genetic

- algorithm for multi-objective optimization: NSGA-II”, *Proceedings of the Parallel Problem Solving from Natural PPSN VI*, Paris, France.
- Duffie, J.A. and Beckman, W.A. (1991), *Solar Engineering of Thermal Processes*, 2nd Edition, John Wiley and Sons Inc., New York, U.S.A.
- Goldberg, D.E. (1989), *Genetic Algorithms in Search, Optimization, and Machine Learning*, Addison-Wesley, Berkshire, U.K.
- Guo, C., Ji, J., Sun, W.M.J., He, W. and Wang, Y. (2015), “Numerical simulation and experimental validation of tri-functional photovoltaic/thermal solar collector”, *Energy*, **3**, 1-11.
- Holland, J.H. (1992), *Adaptation in Natural and Artificial Systems*, MIT Press, Cambridge, U.S.A.
- Ibrahim, A., Othman, M.Y., Ruslan, M.H., Mat, S. and Sopian, K. (2011), “Recent advances in flat plate photovoltaic/thermal (PV/T) solar collectors”, *Renew. Sustain. Energy Rev.*, **15**(1), 352-365.
- Kia, M. (2012), *Genetic Algorithms in MATLAB*, 3rd Edition, KIAN Academic Publications.
- Kroib, A., Präßt, A., Hamberger, S., Spinnler, M., Tripanagnostopoulos, Y. and Sattelmayer, T. (2014), “Development of a seawater-proof hybrid photovoltaic/thermal (PV/T) solar collector”, *Energy Proc.*, **52**, 93-103.
- Lonngren, K.E. and Bai, E.W. (2008), “On the global warming problem due to carbon dioxide”, *Energy Pol.*, **36**(4), 1567-1578.
- Moradi, K. and Ebadian, M.A. (2013), “A review of PV/T technologies: Effects of control parameters”, *J. Heat Mass Trans.*, **64**, 483-500.
- Rejeb, O., Dhaou, H. and Jemni, A. (2015), “A numerical investigation of a photovoltaic thermal (PV/T) collector”, *Renew. Energy*, **77**, 43-50.
- Saeedi, F., Sarhaddi, F. and Behzadmehr, A. (2015), “Optimization of a PV/T (photovoltaic/thermal) active solar still”, *Energy*, **2**, 1-11.
- Safari, F. and Ataie, A. (2015), “Thermal and electrical analysis of a linear parabolic CPVT system”, *Adv. Energy Res.*, **3**(4), 221-233.
- Sobhnamayan, F., Sarhaddi, F., Alavi, M.A., Farahat, S. and Yazdanpanah, J. (2014), “Optimization of a solar photovoltaic thermal (PV/T) water collector based on energy concept”, *Renew. Energy*, **68**, 356-365.
- Srinivas, N. and Deb, K. (1994), “Multi-objective optimization using non-dominated sorting in genetic algorithms”, *J. Evolut. Comput.*, **2**(3), 221-248.
- Tyagi, V.V., Kaushik, S.C. and Tyagi, S.K. (2012), “Advancement in solar photovoltaic/thermal (PV/T) hybrid collector technology”, *Renew. Sustain. Energy Rev.*, **16**(3), 1383-1398.

Appendix

Nomenclature

A	Altitude of observer (km)
A	Surface area of collector side (m^2)
A_c	Surface area of the collector (m^2)
A	Utility coefficient (V)
B	Length of flow line (m)
D	Width of absorber plate on the flow line (m)
E	Semiconductor's band gap energy (J)
F'	Efficiency or output coefficient of collector
G	Solar radiation intensity (W/m^2)
G_b	Beam solar radiation (W/m^2)
G_d	Diffuse solar radiation (W/m^2)
G_{on}	Extraterrestrial radiation flux n incident on the plane normal to the radiation (W/m^2)
G_{sc}	Solar constant (W/m^2)
G_T	Solar radiation on tilted surface (W/m^2)
h_f	Heat transfer coefficient inside the flow path (W/m^2K)
h_{p1}	Punishment coefficient due to presence of photovoltaic cell materials and cell in the PV module
h_{p2}	Punishment coefficient due to presence of tedlar between the fluid and surface of photovoltaic module
h_w	Wind heat transfer coefficient (W/m^2K)
I_L	Electrical current intensity of light (A)
I_o	Reverse saturation current of diode (A)
K_h	Thermal conductivity of absorber plate (W/m^2K)
K_{ins}	Thermal conductivity of insulator (W/m^2K)
L_h	Thickness of absorber plate (m)
L_{ins}	Thickness of insulator (m)
M	Number of flow lines
N	Number of glass covers
N_c	Number of photovoltaic cells in series
Q	Electric charge (A)
R_s	Series resistance (Ω)
T_{amb}	Ambient temperature (K)
T_{bs}	Temperature of absorber plate (K)
T_c	Operation temperature of photovoltaic cell (K)
T_{cm}	Average cell temperature (K)
T_f	Average temperature of fluid(K)
T_{ref}	Reference temperature ($^{\circ}C$)
U	Loss coefficient of corner (W/m^2K)
U_b	Losses from back of the collector (W/m^2K)

U_e	Losses from the sides of collector (W/m ² K)
U_L	Total heat loss coefficient (W/m ² K)
U_s	Losses from top of collector (W/m ² K)
U_T	Total heat transfer coefficient of PV cell to absorber plate (W/m ² K)
U_t	Total heat transfer coefficient of PV cell to ambient environment (W/m ² K)
U_{iT}	Total heat transfer coefficient between the upper level and absorber plate (W/m ² K)
W	Spacing between two adjacent flow lines (m)

Greek Symbols

a_{cell}	Absorption coefficient of photovoltaic cell
a_T	Absorption coefficient of absorber layer
$(a\tau)_{eff}$	Product of effective absorption and transfer
β_{cell}	Compressibility of photovoltaic cell
B	Collector inclination (degrees)
η_{el}	Electrical efficiency of photovoltaic module
ρ_g	Diffuse reflectance constant
η_{mp}	Cell efficiency at point of maximum power
$\eta_{mp,ref}$	Cell efficiency point of maximum power under reference conditions
η_{ov}	The overall efficiency of the system
η_{th}	Thermal efficiency
$\mu_{I,sc}$	Temperature coefficient of electrical current (A/K)
$\mu_{v,oc}$	Temperature coefficient of voltage (V/K)
$\mu_{n,mp}$	Temperature coefficient of photovoltaic cell efficiency
τ_c	Cell transmissivity
τ_g	Transmissivity of glass cover
Δ	Solar declination angle (Degree)
Ω	Hour angle (Degree)
Φ	Latitude angle (Degree)
τ_b	Atmospheric transmittance for beam radiation